archives
of thermodynamics
Vol. **34**(2013), No. 4, 3–21
DOI: 10.2478/aoter-2013-0026

Mathematical model of a plate fin heat exchanger operating under solid oxide fuel cell working conditions

JAKUB KUPECKI[1*]
KRZYSZTOF BADYDA[2]

[1] Fuel Cell Department, Institute of Power Engineering, Augustowka 36, 02-981 Warszawa, Poland

[2] Institute of Heat Engineering, Warsaw University of Technology, Nowowiejska 21/25, 00-665 Warszawa, Poland

Abstract Heat exchangers of different types find application in power systems based on solid oxide fuel cells (SOFC). Compact plate fin heat exchangers are typically found to perfectly fit systems with power output under 5 kW_{el}. Micro-combined heat and power (micro-CHP) units with solid oxide fuel cells can exhibit high electrical and overall efficiencies, exceeding 85%, respectively. These values can be achieved only when high thermal integration of a system is assured. Selection and sizing of heat exchangers play a crucial role and should be done with caution. Moreover, performance of heat exchangers under variable operating conditions can strongly influence efficiency of the complete system. For that reason, it becomes important to develop high fidelity mathematical models allowing evaluation of heat exchangers under modified operating conditions, in high temperature regimes. Prediction of pressure and temperatures drops at the exit of cold and hot sides are important for system-level studies. Paper presents dedicated mathematical model used for evaluation of a plate fin heat exchanger, operating as a part of micro-CHP unit with solid oxide fuel cells.

Keywords: Plate fin; Heat exchanger; Micro-CHP; SOFC, Modeling

*Corresponding Author. E-mail: jakub.kupecki@ien.com.pl

Unauthenticated | 89.73.89.243
Download Date | 3/3/14 12:31 PM

Nomenclature

A	–	area, total fin and wall convection area of a heat exchanger
A_C	–	free-flow area in a heat exchanger
A_f	–	frontal area in a heat exchanger
A_w	–	uncovered wall area taking part in a heat exchange
C_p	–	specific heat capacity
C_r	–	heat capacity ratio
CFC	–	curve fit coefficient used to determine Colburn factor
CFE	–	curve fit exponent used to determine Colburn factor
δ_p	–	pressure drop
ΔT_{log}	–	logarithmic temperature difference
D_h	–	hydraulic diameter
f_C	–	core friction factor
FFC_c	–	friction factor curve coefficient
FFC_e	–	friction factor curve exponent
h	–	heat convection coefficient
j	–	Colburn factor
k_{int}	–	interconnect thermal conductivity
k^{eff}	–	effective thermal conductivity
K_c	–	contraction pressure loss coefficient
K_e	–	expansion pressure loss coefficient
L	–	length of a heat exchanger fin, flow length
m	–	mass flow
Nu	–	Nusselt number
NTU	–	number of transfer units factor
p	–	pressure
Pr	–	Prandtl number
R	–	universal gas constant
R_{th}	–	thermal resistance
Re	–	Reynolds number
St	–	Stanton number
t	–	thickness of a heat exchanger fin
T	–	temperature
V	–	velocity

Greek symbols

ε	–	effectiveness of a heat exchanger
ε_0	–	initial gues for iterative determination of effectiveness of a heat exchanger
μ	–	fluid viscosity
ρ	–	fluid density
σ	–	ratio of free-flow area to the frontal area in a heat exchanger
σ_i	–	contraction coefficient for the heat exchanger inlet
σ_e	–	expansion coefficient for the heat exchanger outlet

Unauthenticated | 89.73.89.243
Download Date | 3/3/14 12:31 PM

Subscripts

in	–	value of a parameter at the inlet
out	–	value of a parameter at the outlet
C	–	cold section of a heat exchanger
H	–	hot section of a heat exchanger

1 Introduction

Several technologies are currently under consideration for highly efficient micro- and small-scale combined heat and power (CHP) units. Typically, internal combustion engines, gas turbines, Stirling engines and fuel cells are listed among the most promising technologies. Special attention has been drawn to micro-CHP generators with power output under 5 kW_{el} [1].

Among the available and emerging technologies, fuel cells are often listed as the units exhibiting the best performance [2]. Four main types of fuel cells are known:

- polymer fuel cell (PEFC),
- phosphoric acid fuel cell (PAFC),
- solid oxide fuel cell (SOFC), and
- molten carbonate fuel cell (MCFC).

Out of the listed, PEFC and SOFC are suitable for micro-combined and power systems. The former exhibits favourable properties for operation under continuous cycling, and in off-design. The latter allows achieving higher electrical and overall efficiencies, however solid electrolytes are prone to degradation caused by power cycling [3, 4]. In general, SOFC-based systems are designed to operate steadily, without major variations of the electrical and thermal load [5]. Additional benefit offered by SOFCs is the ability to operate with large variety of fuels including alcohols [6], hydrocarbons [7], pure hydrogen [7, 9, 10], biofuels [8] and alternative energy carriers which can be converted to hydrogen-rich gas, including ammonia [11] and dimethyl ether [12].

2 Micro-combined heat and power systems with solid oxide fuel cells

Typical micro-CHP system comprises several components allowing highly efficient operation in the design point and in off-design. Example of such

Unauthenticated | 89.73.89.243
Download Date | 3/3/14 12:31 PM

power unit can be seen in Fig. 1. The core of a system is a fuel cell stack. Steam reformer allows conversion of a raw fuel into hydrogen-rich gas fed to the anodic compartments of the stack. Air is supplied to the cathodic side using a micro-air blower.

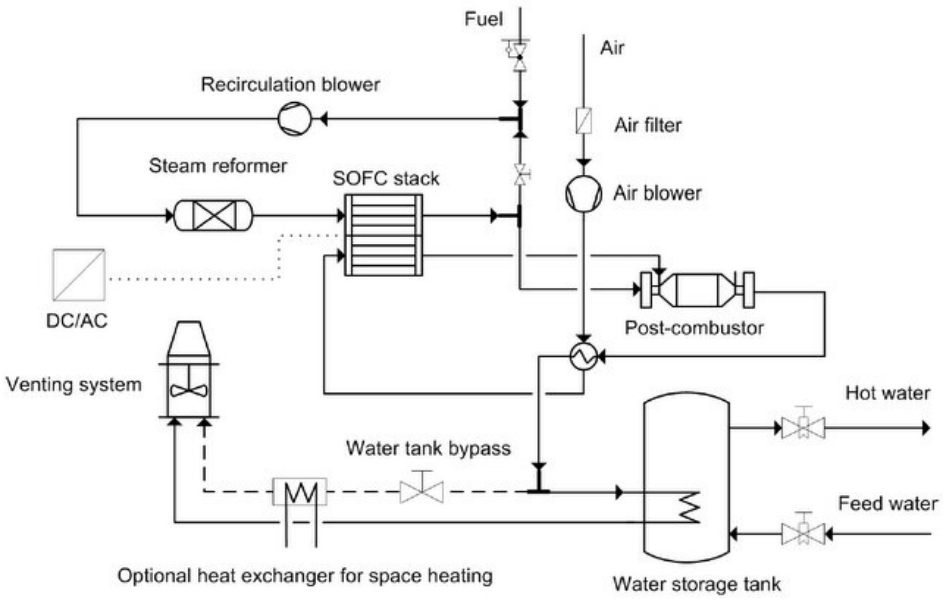

Figure 1. Scheme of a micro-CHP system with solid oxide fuel cells.

Fuel conversion into electricity is never completed in SOFCs. Typically, fuel utilization in range 0.70–0.85 is chosen in a fully operational system [13]. Lean fuel leaving the stack is directed to the post-combustor. Remaining energy can be therefore recovered and used for preheating gases entering the fuel cells. Partial recirculation of anodic off-gas is required to supply sufficient amount of steam to the fuel processor in order to achieve high conversion of fuel and prevent from carbon formation within the system. Heat exchanger is used for preheating air from 283 up to 923 K, which is a typical inlet temperature of a cathode of a SOFC stack. Once the heat of gases exiting the post-combustors is partially recovered to preheat the air stream it can be directed to the hot water storage tank equipped with the heating coil. Alternatively, flue gases can be used to support space heating system using a dedicated heat exchanger (shown in Fig. 1). Main features of the micro-CHP system with solid oxide fuel cells were discussed in detail in previous paper [14]. All of these components exhibit different character-

Unauthenticated | 89.73.89.243
Download Date | 3/3/14 12:31 PM

istics, strongly influencing electrical and overall efficiencies of a micro-CHP system under variable operating conditions. Operation of the SOFC stack influences all auxiliaries. Strong effects of the pressure losses within the system can shift the optimal operating point of the complete system from the SOFC stand-alone optimum. Authors' evaluation indicated that the heat exchanger operating in high temperature zone strongly contributes to pressure losses in the power unit. High sensitivity of pressure losses in the system to variable oxidant utilisation in the fuel cell stack can be explained by large variations of air flow through the hot section of the heat exchanger. For these reasons, dedicated model of a compact heat exchanger operating in a steady state reference conditions was established. The model comprises several geometrical and design-based parameters which are either proprietary data or have to be determined experimentally.

In order to analyse the response of the system to the change of SOFC operating conditions, the complete simulator of the system was required, including the incorporated model of a plate fin heat exchanger. Several alternative mathematical descriptions of heat exchangers are available [15]. Models of compact micro-heat exchanger exists [16,17], and can be adopted and implemented in a simulator of micro-CHP systems which incorporate such heat exchangers. This mathematical description allows prediction of a heat exchanger performance under variable operating conditions, including off-design, in high temperature regimes. Pressure drops in the hot and cold side, and temperatures of gases exiting the unit can be precisely estimated. In addition, model can be used to generate performance characteristics of a particular configuration of a heat exchanger, if needed.

In general, mathematical description introduced in this paper compiles several approaches. This allows to include specific parameters corresponding to the design of this particular heat exchangers. Some of the coefficients used in modeling of the heat exchanger were supplied by the manufacturer as proprietary data, therefore will not be presented in this dissertation.

The proposed mathematical model of an adiabatic heat exchanger is solved iteratively, and requires an initial guess for the effectiveness, ε_0. Since the mathematical model of a heat exchanger is based on the iterative calculation procedure, in the first iteration initial guess for the effectiveness of heat exchanger, ε_0, is used. In the next iteration, final value of the effectiveness is used as a initial guess for the next iteration. This procedure continues until sufficient convergence is obtained. It was found that typically 5–7 iterations are sufficient to achieve differences between iterations

Unauthenticated | 89.73.89.243
Download Date | 3/3/14 12:31 PM

lower than 0.5%. Based on this guess, hot and cold sides of the heat exchanger can be analysed and evaluated, to determine the main parameters at the outlets of both sides. Performance can be evaluated for pure gases and their mixtures. Such parameters as density, specific heat capacity, and viscosity of gas mixtures are calculated using dedicated approximate functions or can be found in thermodynamic tables. In the currently analysed system, heat exchange takes place in a single (gaseous) phase. Proper correlations can be however introduced to extend the functionality of model to multiphase flows. Working fluids, including gas mixtures are modeled using Peng-Robinson equation of state. Specific heat capacities used in this model are found for the average temperatures computed as the arithmetic mean value of the inlet and outlet temperatures. The averaging based on computing specific heat capacity for the mean temperature gives more precise estimate in comparison with finding the value as an arithmetic mean of the inlet and outlet specific heat capacity [19].

3 Model of a plate fin heat exchanger

The model presented in this sections covers various effects typical for the inlet, core and outlet sections of a heat exchanger (Fig. 2). Each of the sides of a heat exchanger are analyzed separately, and main parameters are found for the hot and cold sections.

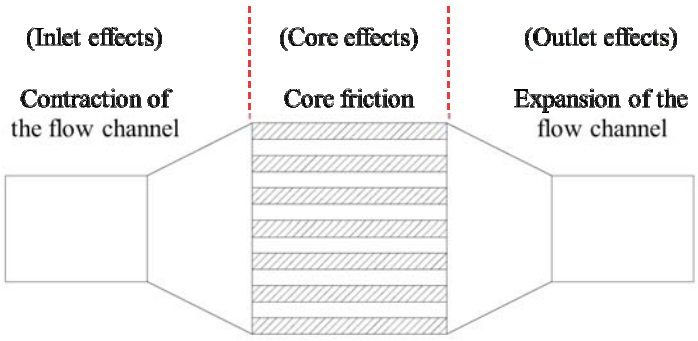

Figure 2. Scheme of a heat exchanger showing main sections of the unit.

Unauthenticated | 89.73.89.243
Download Date | 3/3/14 12:31 PM

3.1 Analysis of the hot side

Temperature at the outlet of a hot side, $T_{H,out}$, can be found, based on the effectiveness of a heat exchanger, ε, and inlet temperatures of the hot and cold sides, $T_{H,in}$ and $T_{C,in}$, respectively. The definition of effectiveness for a counter-flow heat exchanger

$$\varepsilon_0 = \frac{T_{H,in} - T_{H,out}}{T_{H,in} - T_{C,in}} \,, \tag{1}$$

can be transformed into a form which allows determing outlet temperature of the hot side (2).

$$T_{H,out} = T_{H,in} - \varepsilon_0 \left(T_{H,in} - T_{C,in}\right) \,, \tag{2}$$

where in the first iterative step $\varepsilon \equiv \varepsilon_0$.

In a similar manner, outlet temperature of the cold side ($T_{C,out}$) can be found as

$$T_{C,out} = T_{C,in} + \varepsilon_0 \left(T_{H,in} - T_{C,in}\right) \,, \tag{3}$$

originating from

$$\varepsilon_0 = \frac{T_{C,out} - T_{C,in}}{T_{H,in} - T_{C,in}} \,, \tag{4}$$

and the average temperature in the hot side ($\tilde{T}_H$) is computed as

$$\tilde{T}_H = \frac{T_{H,in} + T_{H,out}}{2} \,. \tag{5}$$

Amount of heat extracted from the hot side (Q_H) is found taking into account the mass flow of gas (m_H) present in the hot side, and its specific heat capacity

$$Q_H = m_H C_{p,H} \left(T_{H,in} - T_{H,out}\right) \,. \tag{6}$$

$C_{p,H}$, where $C_{p,H} = f\left(\tilde{T_H}\right)$. An average temperature of the cold side is then calculated as an arithmetic average of the inlet and outlet

$$\tilde{T}_C = \frac{T_{C,in} + T_{C,out}}{2} \,. \tag{7}$$

Heat gain into the cold side Q_C is found as

$$Q_C = m_C C_{p,C} \left(T_{C,out} - T_{C,in}\right) \,, \tag{8}$$

Unauthenticated | 89.73.89.243
Download Date | 3/3/14 12:31 PM

where $C_{p,C} = f\left(\tilde{T_C}\right)$ and m_C is the mass of cold fluid. Maximum amount of heat exchanged between the sides of a heat exchanger Q_{max} can be found as

$$Q_{max} = \left[\min\left(m_H C_{p,H}, m_C C_{p,C}\right)\right]\left(T_{H,in} - T_{C,in}\right) \ . \tag{9}$$

Average density of gas at the hot side are computed using thermodynamic functions. Average gas velocity is calculated as

$$\tilde{V}_H = \frac{m_H}{\tilde{\rho}_H A_{C,H}} \ , \tag{10}$$

where $A_{C,H}$ is the geometry and design depended free-flow area in the hot side. The average Reynolds number ($\tilde{\mathrm{Re}}_H$) is calculated using the average density ($\tilde{\rho}_H$), velocity ($\tilde{V}_H$) and hydraulic diameter of the hot side $D_{h,H}$ in the hot side of a heat exchanger matrix:

$$\tilde{\mathrm{Re}}_H = \frac{\tilde{\rho}_H \tilde{V}_H D_{h,H}}{\tilde{\mu_H}} \ , \tag{11}$$

where $\tilde{\mu}_H$ is the average dynamic viscosity of gas present in the hot side. Density of the gas at inlet of hot side ($\tilde{\rho}_H$) is again, found using thermodynamic functions for gas mixtures. The cumulative pressure drop in the hot side of a heat exchanger is found as a sum of pressure drops due to the entrance effect, fluid acceleration, exit effect and the core friction:

$$\Delta p_{H,HTX} = \Delta p_{H,entrance} + \Delta p_{H,acceleration} + \Delta p_{H,exit} + \Delta p_{H,corefriction} \ . \tag{12}$$

Several relations can be adopted from the thermohydraulics of nuclear systems, since similar operating conditions and geometrical scales are considered [20]. Entrance effect pressure drop in the hot side is found as

$$\Delta p_{H,entrance} = \frac{\rho_{H,in} V_{H,in}^2}{2}\left(1 - \sigma_{in,H}^2 + K_{c,H}\right) \ , \tag{13}$$

where $\sigma_{in,H}$ is the ratio of free-flow area, $A_{C,H}$, to the frontal area, $A_{f,H}$, at the inlet passage contraction ratio, $K_{c,H}$ is the contraction pressure loss coefficient, and $\rho_{H,in}$, $V_{H,in}$ are the density and velocity of hot fluid, respectively. Depending on the design of a heat exchanger, contraction coefficient may substantially contribute to pressure losses [17]. All these parameters describe geometrical properties of the hot side of a heat exchanger. Flow acceleration pressure drop is computed using the following equation:

$$\Delta p_{H,acceleration} = \rho_{H,out}^2 V_{H,in}^2 \left(\frac{1}{\rho_{H,out}} - \frac{1}{\rho_{H,in}}\right) \ , \tag{14}$$

Unauthenticated | 89.73.89.243
Download Date | 3/3/14 12:31 PM

where $\rho_{H,out}$ is the density of hot fluid. Pressure drop due to the exit effect is computed with respect to the expansion pressure loss coefficient [17]

$$\Delta p_{H,exit} = \frac{\rho_{H,out} V_{H,out}^2}{2} \left(1 - \sigma_{e,H}^2 - K_{e,H}\right) , \tag{15}$$

where $\sigma_{out,H}$ is the ratio of free-flow area to the frontal area at the outlet of the hot side, and $K_{e,H}$ is the expansion pressure loss coefficient for the same side of a heat exchanger, and $V_{H,out}$ is the velocity of hot fluid.

Core friction factor $f_{C,H}$ for the hot side of heat exchanger can be found using the following relation (16) [21]:

$$f_{C,H} = FFC_{c,H} \tilde{\mathrm{Re}}_H^{\,FFC_{e,H}} , \tag{16}$$

where $FFC_{c,H}$ and $FFC_{e,H}$ are the friction factor curve fit coefficient and exponent for the hot side, respectively. These numbers are based on fitting the real performance curve to the theoretical curves presented in diagram of friction factor for different pipe flows under variable flow conditions (so-called Moody diagrams). Details of the friction factor determination can be found in the original paper by Moody [22].

Having found the core friction factor, the pressure drop due to the core friction can be found as

$$\Delta p_{H,corefriction} = 2\tilde{\rho}_H \tilde{V}_H^2 f_{C,H} \frac{L_H}{D_{h,H}} , \tag{17}$$

where L_H is a geometrical parameter determining the flow length in the hot side.

3.2 Analysis of the cold side

In a similar manner, analysis of the cold side can be performed using equations given in the previous section of the paper. Set of the following equations applies to the cold side, with the new index denoting the cold side:

$$\tilde{V}_C = \frac{m_C}{\tilde{\rho}_C A_{C,C}} , \tag{18}$$

$$\tilde{\mathrm{Re}}_C = \frac{\tilde{\rho}_C \tilde{V}_C D_{h,C}}{\tilde{\mu_C}} . \tag{19}$$

Unauthenticated | 89.73.89.243
Download Date | 3/3/14 12:31 PM

The cumulative pressure drop in the cold side of a heat exchanger is found again as a sum of pressure drops due to the entrance effect, fluid acceleration, exit effect and core friction:

$$\Delta p_{C,HTX} = \Delta p_{C,entrance} + \Delta p_{C,acceleration} + \Delta p_{C,exit} + \Delta p_{C,corefriction} \ , \tag{20}$$

where

$$\Delta p_{C,entrance} = \frac{\rho_{C,out} {V_{C,in}}^2}{2} \left(1 - \sigma_{i,C}^2 + K_{c,C}\right) \ , \tag{21}$$

and

$$\Delta p_{C,acceleration} = \rho_{C,out}^2 V_{C,in}^2 \left(\frac{1}{\rho_{C,out}} - \frac{1}{\rho_{C,in}}\right) \ . \tag{22}$$

Pressure drop due to the exit effect is found using formula:

$$\Delta p_{C,exit} = -\frac{\rho_{C,out} V_{C,out}^2}{2} \left(1 - \sigma_{e,C}^2 - K_{e,C}\right) \ . \tag{23}$$

Core friction factor of the cold side of a heat exchanger $f_{C,C}$ can be computed using analogical formula as previously

$$f_{C,C} = FFC_{c,C} \tilde{\mathrm{Re}}_C^{\ FFC_{e,C}} \ , \tag{24}$$

and similarly the pressure drop due to the core friction

$$\Delta p_{C,corefriction} = 2\tilde{\rho}_C \tilde{V}_C^2 f_{C,C} \frac{L_C}{D_{h,C}} \ , \tag{25}$$

where L_C is a geometrical parameter determining the flow length in the cold side.

Final evaluation of the heat exchanger includes calculation of the heat transfer effectiveness for both the hot and cold side. In order to evaluate the heat exchange process, main average dimensionless numbers to be determined. As proposed by Kays and London [17], analysis of a compact heat exchanger can be performed using a dedicated methodology. In the proposed design-based approach, heat transfer surface is referred to the total surface of one side of a heat exchanger. The experimental procedure was used to established the correlation and it has been used ever since.

Determination of the Stanton number (St) uses Colburn factor j, which is a product of Stanton number and Prandtl number (Pr) to the power of 2/3,

$$j_H = \tilde{\mathrm{St}}_H \tilde{\mathrm{Pr}}_H^{2/3} = CFC \ \tilde{\mathrm{Re}}_H^{CFE} \ , \tag{26}$$

Unauthenticated | 89.73.89.243
Download Date | 3/3/14 12:31 PM

where CFC and CFE are the curve fit coefficient and curve fit exponent used to determine the value of Colburn factor j, therefore

$$\tilde{\mathrm{St}}_H = \frac{j_H}{\tilde{\mathrm{Pr}}_H^{2/3}} , \tag{27}$$

and

$$\tilde{\mathrm{Pr}}_H = \frac{C_{p_H}\tilde{\mu}_H}{\tilde{k}_H} , \tag{28}$$

where $\tilde{k}_H$ is the average thermal conductivity of a gas. Nusselt number is then found as

$$\tilde{u}_H = \tilde{\mathrm{St}}_H\tilde{\mathrm{Re}}_H\tilde{\mathrm{Pr}}_H . \tag{29}$$

Based on the Nusselt number, an average thermal conductivity of gas in the hot side and hydraulic diameter in the heat exchanger matrix, the average hot side heat convection coefficient ($\tilde{h}_H$) can be computed:

$$\tilde{h}_H = \frac{\tilde{u}_H\tilde{k}_H}{D_{h,H}} . \tag{30}$$

Similarly, the same factors can be evaluated for the cold side:

$$j_C = \tilde{\mathrm{St}}_C\tilde{\mathrm{Pr}}_C^{2/3} = CFC\tilde{\mathrm{Re}}_C^{CFE} , \tag{31}$$

$$\tilde{\mathrm{St}}_C = \frac{j_C}{\tilde{\mathrm{Pr}}_C^{2/3}} , \tag{32}$$

$$\tilde{\mathrm{Pr}}_C = \frac{C_{p_C}\tilde{\mu}_C}{\tilde{k}_C} , \tag{33}$$

$$\tilde{u}_C = \tilde{\mathrm{St}}_C\tilde{\mathrm{Re}}_C\tilde{\mathrm{Pr}}_C , \tag{34}$$

$$\tilde{h}_C = \frac{\tilde{u}_C\ \tilde{k}_C}{D_{h,C}} . \tag{35}$$

4 Effectiveness of a plate fin heat exchanger

Eventually, overall surface effectiveness can be calculated for the hot and cold sides. To evaluate the overall heat exchange, the effectiveness of heat

Unauthenticated | 89.73.89.243
Download Date | 3/3/14 12:31 PM

exchange in single fin, both in the hot and cold sides should be first considered [17]:

$$\varepsilon_{H,fin} = \frac{\tanh\left(l\sqrt{\frac{2\tilde{h}_H}{k_f t_f}}\right)}{l\sqrt{\frac{2\tilde{h}_H}{k_f t_f}}} \,, \tag{36}$$

where k_f is the thermal conductivity of a single fin, t_f is the fin thickness, and l is the length of a fin.

Overall surface heat exchange effectiveness can be found for the hot side [17]:

$$\varepsilon_H = 1 - \left(\frac{A_{fin}}{A}\left(1 - \varepsilon_{H,fin}\right)\right) \,, \tag{37}$$

where A_{fin} is the total fin heat convection area, and A is the total fin and wall convection area of a heat exchanger. Analogically, the effectiveness of heat exchange at the cold side can be evaluated [17]:

$$\varepsilon_{C,fin} = \frac{\tanh\left(l\sqrt{\frac{2h_C}{k_f t_f}}\right)}{l\sqrt{\frac{2h_C}{k_f t_f}}} \,, \tag{38}$$

$$\varepsilon_C = 1 - \left(\frac{A_{fin}}{A}\left(1 - \varepsilon_{C,fin}\right)\right) . \tag{39}$$

Thermal resistances can be determined for heat exchange between hot stream and wall ($R_{th_{hs-w}}$) and cold stream-wall ($R_{th_{cs-w}}$) from the expressions [17]:

$$R_{th_{hs-w}} = \frac{1}{\varepsilon_H A\ h_H} \,, \tag{40}$$

$$R_{th_{cs-w}} = \frac{1}{\varepsilon_C A\ h_C} \,/. \tag{41}$$

Additionally, thermal resistance of the wall (R_{th_w}) can be found depending on the material properties of a heat exchanger

$$R_{th_w} = \frac{t_w}{A_w\ k_w} \,, \tag{42}$$

where t_w is the wall thickness, k_w is the thermal conductivity of the wall, and A_w is the uncovered wall area taking part in a heat exchange. Total thermal resistance $R_{th_{tot}}$ is found as a sum of (40), (41) and (42)

$$R_{th_{tot}} = R_{th_{hs-w}} + R_{th_{cs-w}} + R_{th_w} \,. \tag{43}$$

Unauthenticated | 89.73.89.243
Download Date | 3/3/14 12:31 PM

At this stage, the number of transfer units (NTU) method can be applied to calculate heat transfer in a compact counter current heat exchanger [18]. NTU method is applied in a system, where no information about outlet temperatures from the hot and cold sides is available. Maximum possible heat transfer has to be found in order to define the effectiveness of a heat exchanger. This value is computed under assumption that the heat is exchanged in a unit of infinite length. Maximum theoretical difference of a fluid temperature depends on parameters at the inlet of hot and cold sides $T_{max} = T_{H,in} - T_{C,in}$.
Method is based on calculating heat capacity rates, which depend on the mass flow and heat capacity of fluids at each side of a heat exchanger.

The ealier mentioned heat capacity rates are calculated to determine the heat capacity ratio C_r, found as ratio of the minimal, C_{min}, and maximal, C_{max}, heat capacity rates [18]

$$C_r = \frac{C_{min}}{C_{max}} = \frac{\min\left(C_{p,H}m_H, C_{p,C}m_C\right)}{\max\left(C_{p,H}m_H, C_{p,C}m_C\right)} \,. \tag{44}$$

Number of transfer units factor (NTU) depends on the total thermal resistance ($R_{th_{tot}}$) of this heat exchange system, and is computed as:

$$NTU = \frac{\frac{1}{}}{C_{min}} = \frac{\frac{1}{R_{th_{tot}}}}{\min\left(C_{p,H}m_H, C_{p,C}m_C\right)} \,. \tag{45}$$

Finally, effectiveness of a heat exchanger can be computed

$$\varepsilon = \frac{1 - \exp\left(-NTU\left(1 - C_r\right)\right)}{1 - C_r \ \exp\left(-NTU\left(1 - C_r\right)\right)} \,. \tag{46}$$

In the iterative process of evaluating exit parameters of cold and hot sides, value obtained with formula (46) is used as an initial guess for the next iterative step. Calculation procedure is continued until satisfactory convergence is achieved.

Summarising, the method described in this paper allows evaluation of the effectiveness of a heat exchanger taking into account geometrical parameters of both, the hot and cold sides, properties of the working fluids, their mass flows, and pressure drops. Geometrical factors important for the evaluation of effectiveness are listed in equation

$$\varepsilon = f\left(\sigma_i, \sigma_e, K_c, K_e, f_c, L, D_h, t_f, t_w, k_f, k_w, A_f, A, A_w\right) \,. \tag{47}$$

Unauthenticated | 89.73.89.243
Download Date | 3/3/14 12:31 PM

Complete set of parameters is typically provided by a producer of a particular heat exchanger. It should be emphasised that each of the parameters is defined separately both for the hot and cold sides of a heat exchanger. The exact values are computed specifically for a particular design and geometry. Moreover, several properties of the working fluid in the hot and cold sides, dependent on the operational point of the micro-CHP system with SOFC, influence the effectiveness

$$\varepsilon = f\left(m_H, m_C, C_{p,H}, C_{p_C}, \rho_H, \rho_C, \mu_H, \mu_C, T_{H,in}, T_{C,in}\right) \ . \tag{48}$$

5 Validation of the model

Model presented in this paper was validated using preliminary experimental data for air. At the current stage two datasets were used, both collected at fixed temperatures. The purpose of using two fixed temperature levels, of 293 K and 573 K, was to investigate the error of pressure drop predictions. The investigated plate fin heat exchanger installed in the test stand without an insulation is shown in Fig. 3. Experimental setup used in the study is a part of a complete testing station for a micro-CHP power unit. It allows evaluation of the system components operating under variable conditions. Section used for the heat exchanger evaluation allows to adjust the flow of a gas (or gas mixtures), at fixed temperature and pressure. Test bench is equipped with two differential pressure sensors, one on the cold and one on the hot lines. K-type thermocouples allow sensing the temperature during experiments.

Figure 3. The analysed plate fin heat exchanger in the test bench, without insulation.

Unauthenticated | 89.73.89.243
Download Date | 3/3/14 12:31 PM

Comparison of measured data and results obtained from the model can be seen in Fig. 4. Good agreement was observed, and provides evidence

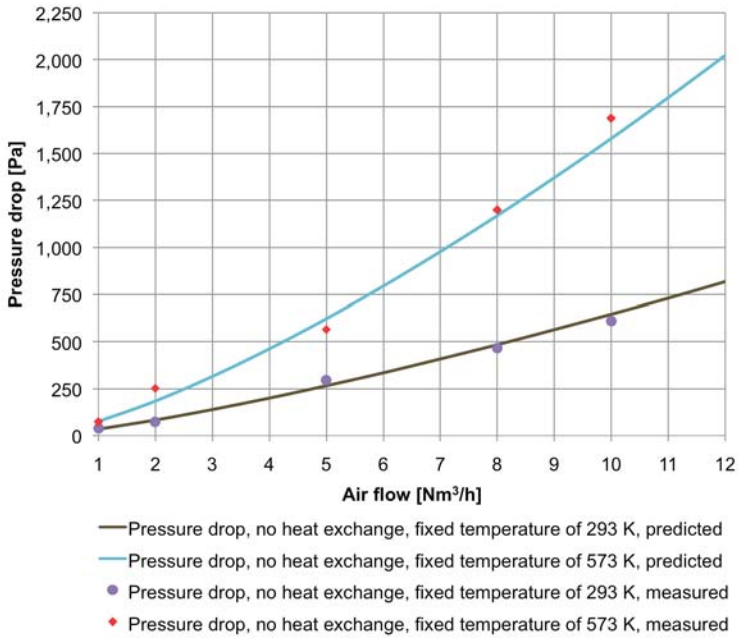

Figure 4. Comparison of experimental data and predictions of the model for pressure drops in a heat exchanger operating at fixed temperature.

that the model can be used for qualitative and quantitative analyses of the plate fin heat exchanger. Slight discrepancy between predictions and measurements can be explained by the nonadiabatic character of the real unit, and uncertainty of the experimental analysis.

Upon successful validation of the model, several cases corresponding to the expected operating parameters of a unit were simulated. During steady state operation, gases exiting the SOFC stack are post-combusted and directed to the heat exchanger to preheat the air. In such case, flue gas temperature of about 1073 K should be expected at the inlet of the hot section, and ambient temperature (293 K) at the inlet to cold section. These operating conditions were simplified, and it was assumed that air enters both sides of a heat exchanger, and the flow varies in range 1–15 Nm^3/h. Based on the additional calculations, heat capacity of nitrogen-rich flue gases differs from the air less than 10% at the elevated temperature. Prediction of the outlet temperatures and pressure drops in hot and cold

Unauthenticated | 89.73.89.243
Download Date | 3/3/14 12:31 PM

sides were plotted against the air flow (Fig. 5). The slope of the pressure drop curves indicates that a loss up to 4900 Pa can be expected in the hot section of a heat exchanger, operating with inlet temperature of 1073 K. In comparison, pressure drop in the cold section increases together with the medium temperature, and can reach 3000 Pa. Pressure drop increase following temperature reduction in the hot section can be explained by the rapid increase of the working fluid volume.

The observed temperature and pressure drop profiles can be potentially used to redesign the power system incorporating compact plate fin heat exchangers. Upon the calculations, and with respect to the maximal allowed pressure drop, single heat exchanger can be replaced with two units, in order to reduce pressure drop in the system. Such profiles can be generated for various operating conditions, including complex gas mixtures. Precise estimation of the pressure drop in a heat exchanger operating in high temperature regime might become a crucial factor from the design optimization point of view.

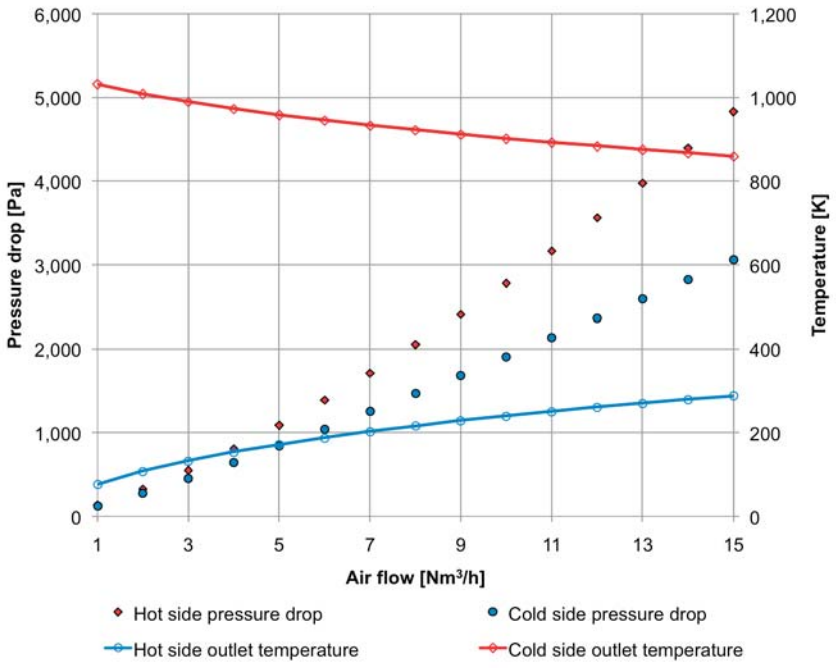

Figure 5. Prediction of the pressure drops and outlet temperatures of the hot and cold sides of a heat exchanger.

Unauthenticated | 89.73.89.243
Download Date | 3/3/14 12:31 PM

6 Conclusions

Effectiveness of a single fin, hot/cold side surface, and the whole heat exchanger can be evaluated using the given equations, with relatively low prediction error. Based on the collected data, the mean squared error was calculated and accounted for 7.3%. This number is a general indicate of the precision of this model in particular conditions. In order to precisely evaluate the model in other operational points, several sets of experiments, each with at least ten data points collected, should be completed. The work presented in this paper is however an introductory phase of the study.

Model finds application in the stand-alone and system-level evaluations of main operating parameters of a plate fin heat exchanger. The particular application, included in the current study, corresponds to the advanced highly efficient micro-combined heat and power system. Operating conditions, imposed by the operational characteristics of a solid oxide fuel cell stack, lay beyond temperature of 973 K. Heat exchange takes place in a single phase, and the typical working media include air and gas mixtures. Due to the complete combustion in the post-combustor, combustible gases are absent in the heat exchanger. Model presented in this paper can be extended to account for complex gas mixtures, including multiphase flows, if needed. The functionality of the model allows predicting performance for complex gas mixtures, and determining simultaneously exit conditions for both the cold and the hot side. Moreover, presented model can be used in two alternative configurations, in exact counter- and co-flow, after minor modifications.

Validation performed at fixed operating temperature allowed to compare pressure drops obtained from the model, using real data. Good agreement was observed.

Acknowledgements This work has been financially supported in frame of Didactic Development Programme of the Faculty of Power and Aeronautical Engineering of Warsaw University of Technology financed within the Operational Programme Human Resources, and Strategic Project Advanced Energy Generation Technologies – Development of integrated energy and fuel generation technologies based on biomass, waste and other resources.

Received 14 October 2013

Unauthenticated | 89.73.89.243
Download Date | 3/3/14 12:31 PM

References

[1] Kirubakaran A., Jain S., and Nema R.K.: *A review of fuel cell technologies and power electronic interface*. Renew. Sust. Energ. Rev. **13**(2009), 2430–2440.

[2] Blum L., Deja R., Peters R., and Stolten D.: *C*omparison of efficiencies of low, mean and high temperature fuel cell systems. Int. J. Hydrogen Energ. **36**(2011), 11056–11067.

[3] Kendall K., Finnerty C.M., Tompsett G.A., Windibank P., and Coe N.: *Rapid heating SOFC system for hybrid applications.* Electrochemistry **68**(2000), 6, 403–406.

[4] Bujalski W. Paragreen J., Reade G., Pyke S., and Kendall K.: *Cycling studies of SOFCs.* J. Power Sources **157**(2006), 745–749.

[5] Sarantaridis D. and Atkinson A.: *Redox cycling of Ni-based solid oxide fuel cell anodes: A review.* Fuel Cells **7**(2007), 3, 246–258.

[6] Jiang Y. and Virkar A.V.: *A high performance, anode-supported solid oxide fuel cell operating on direct alcohol.* J. Electrochem. Soc. **148**(2001), 7 A706–A709.

[7] US Department of Energy Office of Fossil Energy National Energy Technology Laboratory. *Fuel Cell Handbook*, 7th Edn. EG G Technical Services, Inc., 2004.

[8] Staniforth J. and Ormerod R.M.: *Running solid oxide fuel cells on biogas.* Ionics **9**(2003), 5-6, 336–341.

[9] Yokokawa H.: *Understanding materials compatibility.* Ann. Rev. Mater. Res. **33**(2003), 581–610.

[10] O'Hayre R., Cha S.W., Colella W., and Prinz F.: *Fuel cell fundamentals.* Wiley, 2005.

[11] Wojcik A., Middleton H., Damopoulos I., and Van Heerle J.: *Ammonia as a fuel in solid oxide fuel cells.* J. Power Sources **118**(2003), 1-2, 342–348.

[12] Murray E.P., Harris S.J., and Jen H.: *Solid oxide fuel cells utilizing dimethyl ether fuel.* J. Electrochem. Soc. **149**(202), A1127–A1131.

[13] Kupecki J., Jewulski J., and Milewski J.: *Clean Energy for Better Environment*. Chap. Multi-level Mathematical Modeling of Solid Oxide Fuel Cells, 53–85. Number DOI: 10.5772/50724. Intech, Rijeka, 2012.

[14] Kupecki J., Badyda K.: *SOFC-based micro-CHP system as an example of efficient power generation unit.* Arch. Thermodyn. **32**(2011), 3, 33–43.

[15] Badyda K.: *Selected aspects of mathematical modeling of power systems.* Prace naukowe Politechniki Warszawskiej, **189**. Oficyna Wydawnicza Politechniki Warszawskiej, Warszawa 2001.

[16] Munzberg H.G and Kurzke J.: *Gas Turbines – Performance and Optimization.* Springer-Verlag, 1977 (in German).

[17] Kays W.M. and London A.L.: *Compact Heat Exchangers*, 3rd Edn. McGraw-Hill, New York 1984.

[18] Incropera F.P and DeWitt D.P.: *Fundamentals of Heat and Mass Transfer*, 3rd Edn. Wiley, New York 1990.

Unauthenticated | 89.73.89.243
Download Date | 3/3/14 12:31 PM

[19] Badyda K. and Miller A.: *Gas Turbines and Power Systems with Gas Turbines*. Kaprint Publishing, 2011 (in Polish).

[20] Anglart H.: *Thermal-hydraulics in Nuclear Systems*. Warsaw University of Technology Publishing House, Warsaw 2013.

[21] Cengel Y.: *Heat and Mass Transfer*. Mc Graw Hull, New York 2007.

[22] Moody L.F.: *Friction factors for pipe flow*. Trans. ASME, **66**(1944), 8, 671–684.

[23] Grew K.N. and Chiu W.K.S.: *A review of modeling and simulation techniques across the length scales for the solid oxide fuel cell*. J. Power Sources **199**(2012), 1–13.

Unauthenticated | 89.73.89.243
Download Date | 3/3/14 12:31 PM